FREE SPACE VSWR METHOD FOR ANECHOIC CHAMBER ELECTROMAGNETIC PERFORMANCE EVALUATION

Brian B. Tian
MI Technologies
1125 Satellite Blvd, Suite 100, Suwanee, GA 30024
btian@mi-technologies.com

ABSTRACT

This paper gives a detailed account of free space Voltage Standing Wave Ratio (VSWR) method. We first review the formulations and terms commonly used in this method. We then discuss errors involved in its direction determination of extraneous signals, contrasting them among plane wave, spherical wave and specular reflection. We highlight issues relating to its application in anechoic chamber electromagnetic performance. Also discussed is the practice of data processing through analyzing a measured VSWR pattern.

Keywords: Anechoic Chamber, Electromagnetic Testing, Evaluation, Quiet Zone, Range

1. Introduction

The free space VSWR method has been an industrial standard for many decades in antenna range electromagnetic performance evaluation [1]. In anechoic chamber evaluations, applications of this method include quiet zone qualification, reflectivity determination and chamber diagnosis [2-6]. This method has its origin in reflection determination from VSWR in a microwave transmission line. Perhaps because of its conceptual simplicity as understood in one dimensional transmission line, its inherent complexity tends to be overlooked when being applied in a three-dimensional anechoic chamber. As a result, application of this method often varies in practice. This paper gives a detailed account of this method, aimed to promote a more uniform practice in its applications.

2. Amplitude Ripples

Assume two electric field waves expressed as,

$$\vec{E}_1 = E_1 \cos(\omega t + \phi_1) \qquad (1a)$$

$$\vec{E}_2 = E_2 \cos(\omega t + \phi_2) \qquad (1b)$$

where $\omega = 2\pi f$. ϕ_1 and ϕ_2 are phases that are functions of position in space. Sum of these two waves leads to

$$\vec{E} = E \cos(\omega t + \phi\ ) \qquad (2a)$$

Its amplitude E can be expressed as

$$E = \sqrt{E_1^{\,2} + E_2^{\,2} + 2E_1E_2\cos(\varphi)} \qquad (2b)$$

where $\varphi = \phi_1 - \phi_2$. Plots of E in space depict an interference pattern of waves E_1 and E_2. Converting amplitude E into power in dB, we obtain

$$Power(dB) = 20 \times \log 10(E) \qquad (3)$$

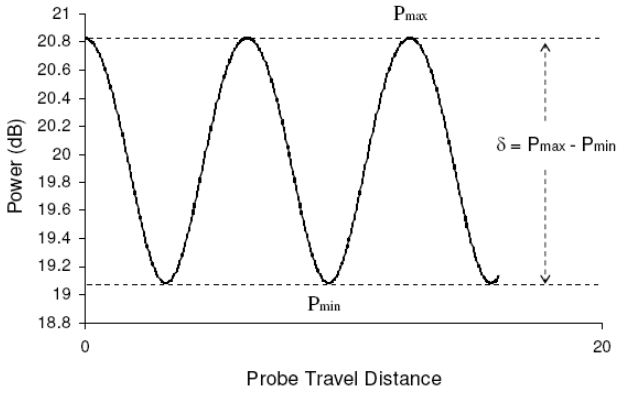

Figure 1. Space interference pattern of two waves (E_1 = 10, E_2 = 1)

As the field probe moves along a line in space, a periodic pattern emerges as shown in Figure 1. In this figure, we take E_1=10 and E_2=1, and φ a linear function of the displacement along the line. According to (2b), a maximum and a minimum occur when

$$E_{\max} = E_1 + E_2 \quad \text{at } \varphi = 2n\pi \quad \text{(in phase)}$$

and

$$E_{\min} = E_1 - E_2 \quad \text{at } \varphi = (2n+1)\pi \quad \text{(out of phase)}$$

respectively, where n = 0, 1, 2….N. Ratio of the maximum and the minimum can be expressed as

$$\rho = \frac{E_1 + E_2}{E_1 - E_2} = \frac{1+\Gamma}{1-\Gamma}, \text{ where } \Gamma = \frac{E_2}{E_1} \qquad (4)$$

When designating wave E_1 as the direct signal and wave E_2 as the reflected or extraneous signal, we term Γ to be reflection coefficient and ρ to be VSWR. Both Γ and ρ are more frequently referred to and used in logarithm space, where

$$R(dB) = 20 \times \log(\Gamma) \qquad (5a)$$

$$\delta(dB) = 20 \times \log(\rho) \qquad (5b)$$

R is thus called reflectivity and δ power VSWR, or ripple as is often called in chamber evaluation. A simple algebraic manipulation of (5) relates R to δ as

$$R(dB) = 20 \times \log \frac{10^{\frac{\delta}{20}} - 1}{10^{\frac{\delta}{20}} + 1} \qquad (6)$$

Using values E_1=10 and E_2=1, one obtains this set of values: $\Gamma = 0.1, R = -20dB, \rho = 1.22, \delta = 1.74(dB)$. They show that a reflection of 1/10 in amplitude of a direct signal of electrical field produces a ripple of 1.74dB or a reflectivity of –20dB.

3. Arrival Direction of an Extraneous Signal

3.1 Introduction

Refer to Figure 2. In literature, we often see the following two equations,

$$d_y = \frac{\lambda}{\sin(\theta)} \qquad (7a)$$

and

$$d_x = \frac{\lambda}{2\sin^2(\frac{\theta}{2})} \qquad (7b)$$

Where λ is the wavelength of the two signals, and d_y and d_x is the direct and the extraneous signals interference pattern's periods along y and x axis respectively. θ is the angle between the two signals.

When scanning along x axis, it is called longitudinal VSWR pattern or cut, while along y axis, the transverse pattern or cut. Loosely, extraneous signals coming from a small θ is classified as on-axis signals while from a large θ as wide-angle signals [1].

Equation (7) shows that arrival direction of an extraneous signal is readily determinable with a known λ and the periods d_y or d_x. While values for both d_x and d_y can be measured relatively easily, determination of the arrival angle in practice however is often not as easy as the simple equation (7) implies. This will be explained further in the rest of this section. In order to facilitate the discussions, we will first give a derivation of the equation (7) and its generalization. Results of spherical waves interference and specular reflections will be introduced later to elicit the limitation and errors in using (7) in the direction determination in an anechoic chamber environment.

3.2 Deriving equation (7) and its generalization

Referring to Figure 2, assume that there are two monochromatic plane-waves S1 and S2. Also assume that the phase shifts are all caused by their travel in space.

When scanning along y-axis (transverse) moving from O to P, the phase shifts of S1 and S2 are respectively as

$$\varphi_1 = 0 \text{ and } \varphi_2 = \frac{2\pi}{\lambda}(r2_p - r2_o) = \frac{2\pi}{\lambda} y \sin(\theta) \qquad (8)$$

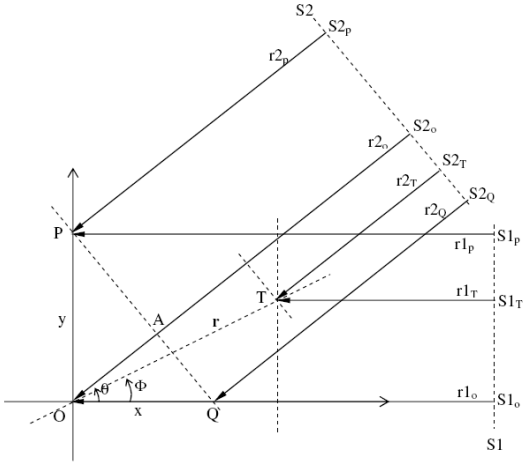

Fig.2 Geometry of two plane-waves S1 and S2 interfering along a line x, y or r in space. θ is the angle between the two waves.

The minimum period of S1 and S2 interference pattern is obtained when

$$\varphi = |\varphi_2 - \varphi_1| = 2\pi \qquad (9)$$

As a result,

$$\varphi = \frac{2\pi}{\lambda} y \sin(\theta) = 2\pi \text{ or } d_y = \frac{\lambda}{\sin(\theta)} \qquad (10)$$

That proves (7a).

When scanning along x-axis (longitudinal), moving from O to Q,

$$\varphi_1 = \frac{2\pi}{\lambda} x \qquad (11a)$$

and

$$\varphi_2 = \frac{2\pi}{\lambda}(r2_Q - r2_O) = \frac{2\pi}{\lambda} x \cos(\theta) \qquad (11b)$$

Similarly, minimum period can be obtained when

$$\varphi = |\varphi_2 - \varphi_1| = \frac{2\pi}{\lambda} d_x (1 - \cos(\theta)) = 2\pi \qquad (12a)$$

That is,

$$d_x = \frac{\lambda}{1 - \cos(\theta)} = \frac{\lambda}{2\sin^2(\frac{\theta}{2})} \qquad (12b)$$

which proves the equation (7b).

Instead having to scan along x or y-axis, one may choose to scan along an arbitrary path of **r** defined by an angle Φ. Following a similar approach, along **r,** we have,

$$\varphi_1 = \frac{2\pi}{\lambda}(r1_T - r1_O) = \frac{2\pi}{\lambda} r \cos(\Phi) \qquad (13a)$$

$$\varphi_2 = \frac{2\pi}{\lambda}(r2_T - r2_O) = \frac{2\pi}{\lambda} r \cos(\theta - \Phi) \qquad (13b)$$

$$\varphi = \frac{2\pi}{\lambda} d_r [\cos(\theta - \Phi) - \cos(\Phi)] = 2\pi \qquad (14a)$$

or $$d_r = \frac{\lambda}{\cos(\theta - \Phi) - \cos(\Phi)} \qquad (14b)$$

where d_r is the period of interference pattern along path **r**.

As a general expression of the interference period along an arbitrary path, equation (14b) readily derives transverse and longitudinal equation of (7), in which (14b) degenerates into (7b) by setting $\Phi = 0$, and (7a) by setting $\Phi = 90^o$ respectively. Further, if letting $\Phi = \theta$, we obtain the case where scan is performed in the direction that coincides with S2 wave's travel direction, a case similar to the situation of x scan, where x scan coincides with the direction of S1 wave's travel direction. It is therefore not surprising that (14b) degenerates into (7b) also in this case.

3.3 Discussion

Equations (7a) and (7b) are plotted in Figure 3. The periods d_x and d_y are normalized by λ. A number of observations can be made from the plot.

1. In acquiring a VSWR pattern, one usually wants to cover at least one complete period with as short a travel distance as possible. From this point of view, a transverse scan, that is, along y axis, is more advantageous than a longitudinal scan in region of small angle. For example, for a period of 5λ, a transverse can detect an incoming wave of 11.5 degrees, while a longitudinal scan can only detect that of 37 degrees. With such large an angle, a longitudinal scan would have missed the entire frontwall for most chambers.

2. On the other hand, only longitudinal scans are suitable for the backwall region, i.e. the region around 180 degree. In this region, as we can see, the period of a transverse pattern is very large. Most practical setups cannot travel the distance of such large a period. Longitudinal patterns, on the other hand, have much smaller periods in this region. For example, it is under one λ from 90 to 270 degree, and only λ/2 at 180 degree.

3 Centering at 90 and 270 degree, the transverse has a broader flat region than longitudinal does, which makes the transverse more advantageous to cover the sidewall reflection.

4. Transverse and longitudinal patterns can be used together to confirm the direction of an extraneous source. For example, when the longitudinal pattern shows a period of 0.53λ while the transverse a period of 2λ, one can be positive that the reflection comes from either 150 or 210 degree.

5. Because of broad angle coverage, either the transverse or the longitudinal can pickup extraneous signals of different angles, registering as multiple periods within a single VSWR pattern. For example, if there are three dominant reflections from 30, 90 and 180 degrees existed in a chamber, a single longitudinal scan would register a period of λ (for the 90 degree reflection) and another of λ/2 (for the 180) assuming it would miss that of 30 degree due to being too large a period to cover, while a single transverse scan registers a period of 2λ (for the 30 degree reflection) and another λ (for the 90 degree).

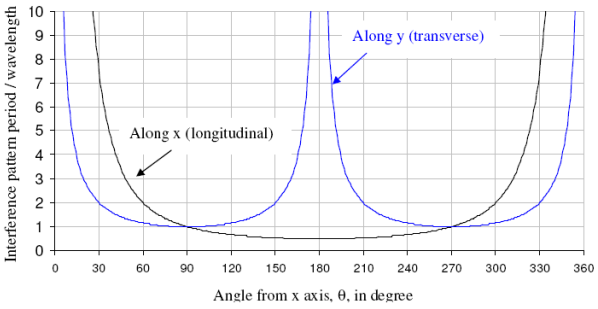

Figure 3. Period in wavelength, λ, of interference pattern along x and y-axis vs. angle θ.

6. When there are many more extraneous sources existing in a chamber, interpretation of a pattern to decipher their directions can be difficult. Use of a highly directive receiving antenna can alleviate some of the problems by limiting the number of extraneous signals coming into the receiver. But sometimes precisely because of the antenna pattern effect, compounded with other issues, direction determination can be made unreliable. One of the issues is related to the model that derives equation (7), which will be discussed next.

3.4 Accuracy in the direction determination

There are many factors affecting the feasibility and the accuracy of using the equation (7) based approach for extraneous signal direction determination. One of the most fundamental comes from the fact that formula (7) is derived based on plane-waves assumption. Dependent on the size and geometry of an anechoic chamber, such assumption is almost always violated to a certain extent. For a direct point source in the chamber, a better model for its propagation is a spherical wave. For a point source reflecting off from a chamber wall, a better model is a spherical wave in conjunction with consideration of specular reflection. In the following, we will compare the directions predicted by plane waves, spherical waves and specular reflection to elucidate the limitation and magnitude of the error of equation (7).

1. Spherical wave

While the interference of two plane waves can be discussed in an infinite plane with the period of interference pattern dependent only on the angle of the two waves involved, two spherical waves interference

pattern depends on the locations of the two sources. Obviously, the combination of locations of the two sources is infinite. To study a case where its result is relevant to our anechoic chamber field evaluation, we choose a geometry shown in Figure 4.

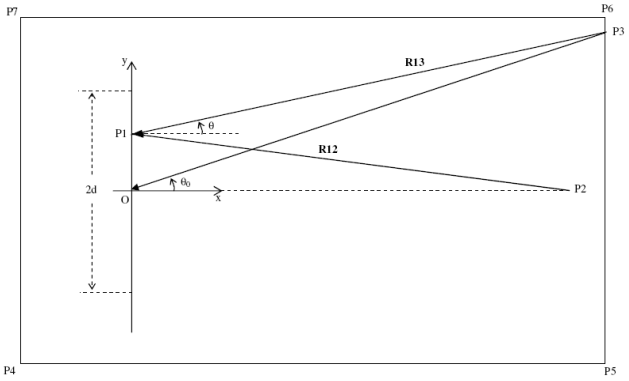

Figure 4 Geometry of two point sources (P2 and P3) interfering at point P1 in a confined rectangular plane defined by P4 to P7. Source P2 can be imagined as a fixed transmitter and P3 as any other extraneous source.

P_2 and P_3 are the two sources and interfere at P_1. P_1 moving along the y axis represents a transverse scan pattern. Moving along the x axis represents a longitudinal scan. θ defines the angle between P_2 and P_3. When P_1 = O, $\theta = \theta_0$. θ_0 will later be contrasted to the angle between two plane waves discussed in the plane waves interfering case. Different from plane wave interference, the angle θ changes as P_1 moves. We use two angles, θ_{max} and θ_{min}, to measure how large the angle has changed over the scan range. θ_{max} is the value of angle θ when Y_1 = -d, that is, one end of the scan range, while θ_{min} is the value of angle θ when Y_1 = d, the other end of the scan range. P_4 through P_7 define the rectangular plane, representing the boundary of an anechoic chamber.

Phases of the two E fields received at point P_1:

$$\phi_1 = \frac{2\pi}{\lambda} R_{12} \text{ and } \phi_2 = \frac{2\pi}{\lambda} R_{13} \qquad (15a)$$

respectively. Their difference

$$\phi = \phi_2 - \phi_1 = \frac{2\pi}{\lambda}(R_{13} - R_{12}) = 2\pi(r_{13} - r_{12}) \qquad (15b)$$

Pattern maxima occur at $\phi = 2n\pi$ (16)

The pattern period on each scan line is defined as the distance between two consecutive n.

2. Specular reflection

Refer to Figure 5. When considering that the phase shift is caused by path length only, we can express Φ_1 and Φ_2 as follows.

$$\Phi_1 = \frac{2\pi}{\lambda} r_1 \text{ and } \Phi_2 = \frac{2\pi}{\lambda}(r_2 + r_3) \qquad (17)$$

$$\phi = \Phi_2 - \Phi_1 \qquad (18)$$

Note that as P1 moves along y or x, reflection point P3 must move accordingly. Therefore resolving equations (17, 18) requires solving simultaneous equations. Also note that there should be a 180 degrees phase added into (17b) to take into account the phase change at the point of reflection.

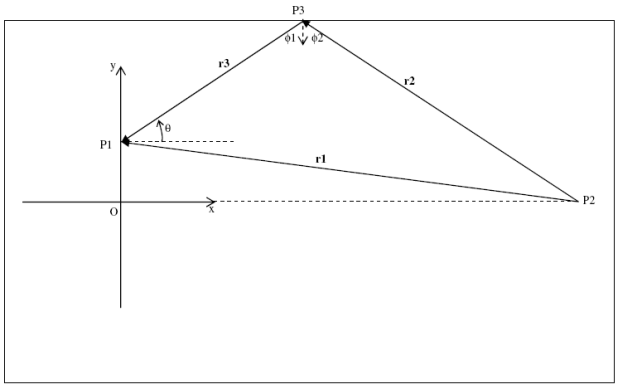

Figure 5 Geometry of specular reflection at P3 with a source at P2, interfering at P1

3. The results

Table 1 and 2 shows the angles comparison among the plane, spherical and specular waves. They show that for given probe travel distance, at around 41 degree for plane wave, the angles can vary by 5 degrees for specular for the transverse travel. For a longitudinal travel, they vary by 12 degrees for spherical waves and 6 degrees for specular reflection.

Table 1. angles at 41 deg (trans)			
	plane	spherical	specular
min	41.000	39.381	38.089
max	41.000	41.241	43.091
average	41.000	40.770	40.762

Table 2. angles at 41 deg (long)			
	plane	spherical	specular
min	41.000	35.725	37.999
max	41.000	47.614	43.877
average	41.000	41.206	40.878

4. Analyzing Measured Interfering Patterns

Refer to Figure 6. The free space VSWR method assumes that direct and reflected waves meet at point P along a line AB on which the probe travels. This method further assumes that amplitude of the receiving signal produces a VSWR pattern, similar to Figure 1, from which its reflectivity can be derived using equation (6). A measured interference pattern, however, is usually much more complex than that depicted in Figure 1, as clearly demonstrated by the bold trace in Figure 7, an interference pattern measured in an actual chamber. Most noticeably,

the trace is not leveled, and the amplitude and periodicity vary significantly along the line of its travel.

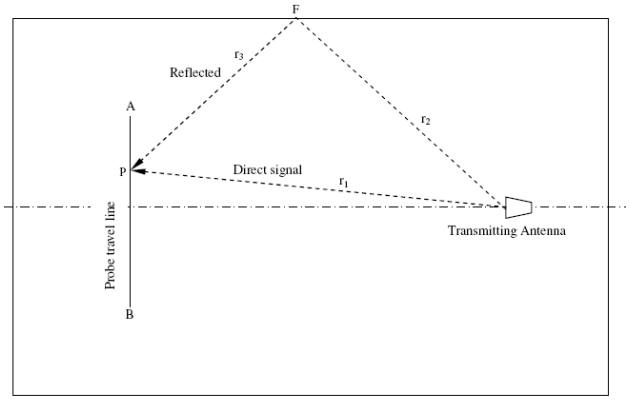

Figure 6 Direct and reflected signals meet along the probe travel line, producing an interference pattern, from which reflectivity is derived.

The significant departure of a measured VSWR pattern from Figure 1 results from the chamber environment violating many assumptions on which Figure 1 is based. These are the key assumptions. First, it assumes that only two coherent waves are present. Secondly, phase difference between the two waves is a linear function of the displacement along line AB. Finally, the amplitudes of the two waves are constant, in this case, $E_1 = 10$ and $E_2 = 1$, along the entire line of probe travel.

An actual chamber may violate all of the above assumptions. Firstly, there may be more than two waves interfering along line AB. Reflections may come from the walls on the left, on the right, from the floor and the ceiling, as well as any objects that reflect inside the chamber. What further complicates the scenario is the fact that, as the probe moves along the line, the locations of some of reflection sources may move simultaneously. Take reflection point F in Fig.6 as an example. As P moves along the line, the law of specular reflection dictates that F moves along a line on the chamber wall. In other word, every time the probe moves, it sees a reflection coming from a different location. As a result, the "two waves" assumption is violated not only because there are potentially more than one reflecting sources, but also because each "one" is not truly a fixed one but many "ones" of different locations as the probe moves along the line. Considering the fact that specular reflection is one of the most simplistic treatments of the electromagnetic wave interactions involved in a chamber wall, the actual pattern can only be much more complicated.

Secondly, the above-mentioned mechanisms inevitably alter the amplitude of the reflections, therefore invalidating the assumption of constant amplitude, contributing to the large variation we see in the amplitude of the measured pattern. In addition, the amplitude of the direct signal may not remain constant either, due primarily to the antenna pattern effect and slightly to the change in r_1. This is the main cause of the overall slope we see in the measured trace.

Finally, phase difference, φ, cannot be a linear function of the probe displacement either. For a simple case of specular reflection, the phase difference caused by phase shift due to the distance changes alone in r_1, r_2 and r_3 resembles more of a 2nd order function of the probe's displacement. This alters both the shape and the periodicity of an interference pattern.

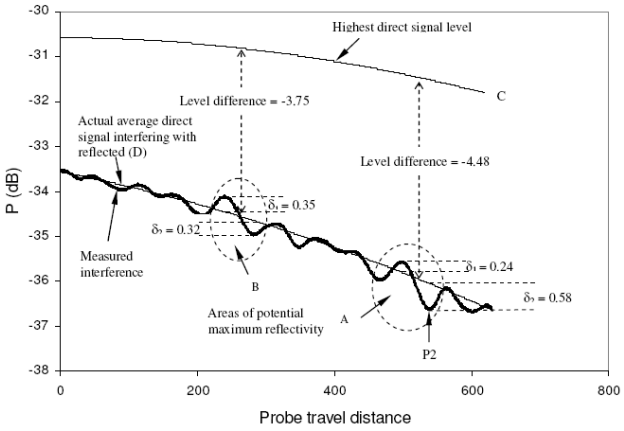

Figure 7 Illustration of a more realistic interference pattern and how the maximum reflectivity value should be determined.

The above discussion influences how we interpret and determine reflectivity. First, because an interference pattern of real chamber usually has an irregular shape, a single pattern can therefore produce more than one values of reflectivity due to its variable amplitude. Take the trace of Figure 7 as an example. By visual inspection, we will find two different reflectivity values at area A and B, and many more at other areas. It has been a common practice that one interference pattern be given only one value of reflectivity. Usually the maximum value is picked. Secondly, a reflectivity does not necessarily quantify the reflection of a particular location or any wall. It is, instead, an indication of overall effect from reflections and extraneous signals of all possible sources and locations. In this sense, it is better to call it ripple of the quiet zone, as the term reflectivity can be misleading.

5. Determining Reflectivity from a Measured Pattern

In this section, we discuss how reflectivity is determined from a measured interference pattern in practice, referring to Figure 7 as example.

The first step is to identify the area of the largest ripple or several of such areas when they are comparable, such as areas A and B. On computing δ, the local slope needs to be removed by finding δ_1 and δ_2 separately. δ is thus the sum of δ_1 and δ_2

$$\delta = \delta_1 + \delta_2 \qquad (19)$$

In Figure 7, δ is measured 0.82 (dB) and 0.67 (dB) respectively for areas A and B. Substituting the values of δ into (6), we obtain two reflectivities,

$R_{rA} = -26.53(dB)$ for area A

$R_{rB} = -28.28(dB)$ for area B

respectively. R_{rA} and R_{rB} may be termed ripple reflectivities since they are the results from ripples only. Final value of reflectivity must include the contribution from over all pattern level differences to be discussed next.

A meaningful reflectivity must be referenced to the maximum direct signal the probe detects. In the case of Figure 7, the direct signal is represented by line C, whose power level is often measured when the receiving and transmitting antennas directly face each other. As the receiving antenna points away, as required by the VSWR procedure, from the transmitter during measurement, the direct signal normally declines steadily.

Final reflectivity is computed as

$$R = R_r + level\_difference \qquad (20)$$

where R_r is ripple reflectivity in dB and level_difference is the power difference in dB between the maximum direct signal and the direct signal that actually interferes with the reflected signal, marked with D in Figure 7. This leads to the final reflectivity at A and B to become

$$R_A = -26.53 - 4.48 = -31.01(dB) \qquad (21a)$$

$$R_B = -28.28 - 3.75 = -32.03(dB) \qquad (21b)$$

respectively. As mentioned earlier, only the largest shall be chosen as the reflectivity, that is, –31.01 dB in this case, occurring at area A where the largest ripple is located.

Even though the largest ripple usually results in a maximum reflectivity, it is however not always true. Depending on the level difference, maximum reflectivity may be obtained at an area where the ripple is not the largest. For instance in Figure 7, had the level difference at area B been –2.00 (dB) rather than –3.75 (dB), R_B would have been –30.28(dB) and overtaken R_A to become the maximum reflectivity. The final reflectivity would have been assigned –30.28 (dB), occurring not at the largest ripple but the 2nd largest.

In order to calculate the level difference and slope effect, one must draw a line of the average direct signal shown as line D. Usually, this line can be well approximated by curve-fitting the interference pattern trace.

When evaluating a chamber using free space VSWR, one may acquire considerable amount of data. Manual data process is time-consuming and often becomes prohibitive. Even more difficult is the task of maintaining consistency throughout the entire process of hundred and thousand of data and patterns. Automation of the above process is highly desirable and often indispensable.

Finally, it needs to point out that we only discussed so far on how a reflectivity shall be determined in a normal situation. There are some important exceptions. One such exception is when an extraneous signal is larger than the direct signal. Another is when features of antenna patterns, for example, nulls, become dominant factors showing up on interference patterns. The former is best identified during the data acquisition period, while the latter can only be analyzed along with their antenna patterns. Therefore, when situation warrants, one should be prepared to take antenna pattern measurement in addition to VSWR patterns.

Acknowledgement

The author wishes to thank Jeffrey A. Fordham and Donald G. Bodnar at MI Technologies for their reviews and comments.

REFERENCES

[1] "IEEE Standard Test Procedures for Antennas", IEEE STD 149-1979.

[2] J. Appel-Hansen, "Reflectivity Level of Radio Anechoic Chambers," IEEE Trans. Antennas Propagat., Vol 21, July 1973, pp 490-498.

[3] E.F.Buckley, "Outline of Evaluation Procedures for Microwave Anechoic Chambers," Microwave Journal, Vol 6, Aug 1963, pp 69-75.

[4] J.S. Hollis, T.J. Lyon and L.Clayton Jr., "Microwave Antenna Measurements," Scientific-Atlanta, Atlanta, GA, 1970.

[5] K. Hatakeyama, H Togawa, T,Kawamura and Y. Sato, "Experimental Study on Direction Dependency of Reflection Coefficients of Microwave Electromagnetic Anechoic Chamber," IEEE Trans. Electrom. Compat. Vol. 34, no, 4, Nov. 1992, pp397-403.

[6] A. Lehto, J. Tuovinen, A. Raisanen, R. Pitkaaho and J. Aurinsalo, "Evaluation of Reflections in Anechoic Chambers at 110 GHz,", AMTA 1989.